JBUON 2017; 22(2): 445-453
ISSN: 1107-0625, online ISSN: 2241-6293 • www.jbuon.com
E-mail: editorial_office@jbuon.com

ORIGINAL ARTICLE

Study on the molecular mechanism of Rac3 on regulating autophagy in human lung cancer cells

Xuyang Xiao[1], Gebang Wang[2], Hongxu Liu[2]

[1]China Medical University, Shenyang, 110122, China; [2]Department of Thoracic Surgery, Liaoning Cancer Hospital and Institute, Shenyang, 110042, China

Summary

Purpose: *Rac3 plays an important role in regulating tumorigenesis. Autophagy plays a vital role in tumorigenesis and tumor progression. The relationship between the two remains unclear. The objective of the present study was to determine the specific molecular mechanism of intracellular Rac3 in regulating autophagy and reveal the relationship between tumor cell autophagy and apoptosis.*

Methods: *A laser confocal microscope was used to photograph the accumulated EGFP-MAP1LC3 spots for investigating the relationship between Rac3 and autophagy at the cellular level. Immunoblotting was also used to investigate the relationship between Rac3 and autophagy. The autophagy flux arising from inhibition of Rac3 was detected with autophagy inhibitors and ATG5 and ATG7 siRNA interference experiments. ATF4 and DDIT4 siRNA interference and overexpression experiments were conducted to investigate the relationship between endoplasmic reticulum stress, the MTOR signaling pathway, and autophagy arising from inhibition of Rac3. Co-immunoprecipitation experiments were performed to investigate the interaction between Rac3 and proteins related to endoplasmic reticulum stress. Co-immunoprecipitation was performed to investigate the structural domains between Rac3 and HSPA5.*

Results: *The expression of ATF4 and DDIT4 was upregulated, which inhibited the MTOR signaling pathway and induced autophagy of human non-small cell lung cancer cells after Rac3 siRNA was introduced. The degree of acetylation of the substrate, HSPA5, increased and the endoplasmic reticulum stress response was activated after Rac3 was inhibited.*

Conclusion: *In conclusion, the degree of acetylation of HSPA5 increased and it was dissociated from the receptor, EIF2AK3, on the endoplasmic reticulum membrane, thus causing the endoplasmic reticulum stress response. Endoplasmic reticulum stress activated the expression of the ATF4 protein, upregulated the level of DDIT4, inhibited the MTOR signaling pathway, and caused cellular autophagy.*

Key words: *autophagy, ATF4, DDIT4, MTOR, Rac3*

Introduction

At present, lung cancer has the highest mortality rate among cancers in the world. The 5-year survival rate is only 14%. Over the last several decades, research on the treatment of non-small cell lung cancer has focused on identification and verification of molecular targets and potential drugs. Autophagy occurs when cells are subject to mitochondrial damage, abnormal accumulation of proteins, hypoxia, bacterial or viral infections, or nutritional deficiency [1]. Autophagy is a conservative catabolic process that degrades damaged organelles and proteins with long half-life periods. It relies on the lysosomal metabolic pathway in eukaryotic cells, thus maintaining metabolic balance of proteins and stability of the intracellular environment [2]. Autophagy is regulated

Correspondence to: Hongxu Liu, MD. No.44 Xiaoheyan road, Dadong District, Shenyang City, Liaoning Province, China.
Tel: +86 24-31916682, Fax: +86 24-24315679, E-mail: al7u92@163.com
Received: 08/10/2016; Accepted: 22/10/2016

by many intracellular signaling pathways, such as the MTOR signaling pathway, the PI3K-AKT signaling pathway, and the Ca^{2+} signaling pathway [3-5]. In tumor cells, the P13K/AKT signaling pathway is activated and the expression of BCL2 is upregulated and binds to BECN1 in an inhibitory manner. In such instances, autophagy is inhibited [6]. In addition, under nutritional deficiency or conditions of external stress, the tumor suppressor gene p53 is activated. Cellular autophagy is further activated by inhibiting MTOR or activating DRAM1 [7]. The overexpression of p62 promotes tumorigenesis [8] by downregulating NF-κB, accumulating reactive oxygen species (ROS), or increasing DNA damage. Deletion of other key autophagy-related genes, such as ATG5 and ATG7, can also lead to tumorigenesis, indicating that blocking autophagy leads to tumorigenesis [9]. Blocking autophagy can substantially increase the occurrence of necrocytosis and inflammation, which are potential causes of tumorigenesis.

Hypoxia and glucose deficiency can lead to activation of AMPK, upregulation of proline dehydrogenase/oxidase (PRODH/POX), and increase of intracellular ROS, thus promoting autophagy of protective A549 lung cancer cells and survival of tumor cells [10,11]. Rac3 (AIB1, SRC-3, NCoA3) is a member of the nuclear receptor co-activation p160 family [12]. The other two members include SRC-1 and TIF-2 [13]. Rac3 was first described as a co-activator of the estrogen receptor or other estrogen receptors [14]. Some studies found that Rac3 is also a co-activator of NF-κB [15]. In general, it has histone transferase activity and can increase the transcriptional activity of the PPAR nuclear receptor [16]. Rac3 was found to be overexpressed in hormone-dependent tumors when initially reported. In recent years, it was also found to be highly expressed in hormone-dependent tumors. It is considered to be an oncogene that promotes cell proliferation by different means [17]. It exerts its functions through nuclear receptors and transcription factors. In recent years, it was found that it exerts an antiapoptotic function by positively upregulating the activity of p38 and AKT [18]. Furthermore, it inhibits Caspase-8 and blocks the translocation of mitochondrial proapoptotic factors to the nucleus [19]. Thus, Rac3 appears to have many different functions. However, the relationship between such functions and autophagy remain unclear.

Given that autophagy and the expression of Rac3 vary with changes of tumor cells, the aim of the present study was to describe the relationship between Rac3 and autophagy, and the underlying mechanism, and determine the relationship between autophagy and apoptosis in tumor cells. This study is expected to serve as a reference for clinical treatment of tumors.

Methods

Transfection with siRNA

Transfection was performed when the density of cultured cells grown in dishes or plates (Calu-1, A549, and H1972; ATCC, Manassas, VA, USA) reached 60–80%. A volume of 3.6 µl of siRNA (Invitrogen Life Technologies Inc., CA, USA) at a concentration of 20 µM was added to 100 µl of culture medium. A total of 5 µl of the transfection reagent (Invitrogen Life Technologies Inc., CA, USA) was added to another 100 µl of culture medium. The two solutions totaling 200 µl were mixed and incubated for 15 min at room temperature. The original culture medium in culture dishes or plates was discarded and replaced with 600 µl of fresh culture medium containing 5% serum (Gibco BRL, Life Technologies Inc., NY, USA). The transfection compounds were added to the culture dishes or plates. They were well mixed by gentle shaking. They were then placed in a carbon dioxide incubator (Thermo Scientific, Waltham, MA) for culture. The culture dishes or plates were shaken several times separated by 15 min intervals. Media were replaced with fresh culture medium containing 5% serum after 6 hrs. Cells were then placed in the carbon dioxide incubator for further culture.

Plasmid transfection

Transfection was performed when the density of cells in culture (H1792, H1299, Calu-1; ATCC, Manassas, VA, USA) reached 60–80%. A total of 1 µg of the plasmid (Polysciences, Inc, Warrington, PA) and 2 µl of the transfection reagent (Invitrogen Darmstadt, Germany) were each added to 100 µl of culture medium. They were well mixed by gently pipetting up and down and incubated for 15–20 min at room temperature. The original culture medium in culture dishes or plates was discarded and replaced with fresh culture medium containing 5% serum. The transfection compounds were added to culture dishes or plates. They were well mixed and cultured in the carbon dioxide incubator. The culture dishes or plates were gently shaken once at an interval of 15 min. The cells continued to be cultured in the carbon dioxide incubator after the original medium was replaced by fresh culture medium containing 5% serum after 8 hrs.

Gene cloning

The target fragments were subject to PCR amplification (details in ref [20]). The polymerase chain reaction (PCR) system was expanded to 30 µl after target

fragments were obtained by PCR. The target fragment gel was recovered. The PCR and cloning vector connection products were subject to dual-enzyme digestion. A total of 2 µl of the connection product was added to 10 µl of DH5α Escherichia coli cells (Science Applications International Co, Frederick, MD). Bacterial cells were well mixed by pipetting up and down, rapidly placed on ice, and allowed to stand for 30 min. They were subject to thermal shock for 90 s at 42°C and then placed on ice for 2 min. A total of 500 µl of Luria-Bertani (LB) liquid culture medium containing 0.1% Ampicillin (Amp) (Hyclone, Logan, UT, USA), was shaken for 1 hr in a constant-temperature shaker at 37°C and 220 rpm. A total of 200 µl of bacterial suspension was added to LB solid plates containing 0.1% Amp (Hyclone, Logan, UT, USA). Plates were cultured overnight at 37°C. A total of 10–20 single colonies were selected for streaking and amplification. All streaked bacterial colonies were subject to electrophoresis. A total of 20 µl sterile water was added to 1.5 ml centrifuge tubes. Sterile water was added to the bacterial colonies in appropriate quantities. They were well mixed by pipetting up and down. A total of 20 µl of phenol/chloroform (Beifang Biotechnology Institute, Beijing, China) was added to centrifuge tubes. They were vortexed for 10 s and centrifuged for 10 min at 16,000 g and 23°C. The bacterial colonies that tested positive for electrophoresis results were subject to PCR. Plasmid extraction and sequencing were performed for the bacterial colonies with available PCR results (Qiagen, Valencia, CA, USA).

Immunoblotting

The human lung cancer cell lines were washed 2–3 times with warm phosphate buffer saline (PBS) after the culture medium was discarded. An appropriate volume of pre-chilled lysis buffer was added (Promega Corp., Madison, WI, USA). Plates were placed on ice for 10–20 min. The cells were harvested with a cell scraper and collected in Eppendorff tubes, and subjected to sonication (Thermo Scientific, Waltham, MA) (100–200 W) twice for 3 s each. Then the cells were centrifuged for 2 min at 12,000 g and 4°C. A small volume of supernatant was used for quantification. A total of 20 µg of protein was loaded in gels and electrophoresed through the stacking and resolving layers of the gel by SDS-PAGE. Next, the two layers of gel were carefully detached following completion of SDS-PAGE. A spongy cushion, a piece of filter paper, the gel, a membrane, a piece of filter paper, and a spongy cushion were assembled in order, for preparation of protein transfer. After bubbles were expelled with a glass rod, the transfer assembly was placed in an electroblotting tank (Thermo Scientific, Waltham, MA) for transferring for 90 min at a voltage of 100 V (350 mA). Following transfer, membranes were placed in dishes containing 25 ml of blocking buffer (Millipore, Billerica, MA) using tweezers and gently shaken for 2 hrs in a decolorization shaker at room temperature. After addition of Rac3 (Abcam, Cambridge, UK), MAP1LC3B (Abcam, Cambridge, UK), ATF4 (Abcam, Cambridge, UK), DDIT4 (Abcam, Cambridge, UK), p-RPS6KB1 (Cell signaling technology, MA, USA), p-EIF4EBP1 (Cell signaling technology, MA, USA), HSPA5 (Cell signaling technology, MA, USA), EIF2AK3 (Cell signaling technology, MA, USA), and acetylated lysine (Cell signaling technology, MA, USA) primary antibodies, membranes were incubated overnight at 4°C and washed three times for 5 min with tris buffered saline (TBST) in a shaker at room temperature. After addition of the secondary antibody (Boster Bioengineering Co., Ltd., Wuhan, China), membranes were incubated on a shaker for 1 hr at 37°C, washed three times with TBST for 5 min, and developed for observation.

Co-immunoprecipitation (IP)

The human lung cancer cells H1792 and H1299 (ATCC, Manassas, VA, USA), were washed once with PBS, harvested, and centrifuged for 5 min at 1,000 g and 4°C. Next, 1 ml of PBS was added to re-suspend the cells after the supernatant was discarded. The cells were transferred to 1.5 ml centrifuge tubes and centrifuged for 5 min at 5,000 g and 4°C. The supernatant was discarded to obtain the cell pellet. Total cellular protein was extracted (similarly as for immunoblotting). Based on the protein concentration obtained, 500–1000 g of protein were used to prepare IP electrophoresis samples. The IP cell lysis buffer containing 1% protease inhibitor (Cotop, Amsterdam, the Netherlands) was added to protein samples until the volume reached 500 µl. A total of 500 µl of protein suspension was added to Protein G-Agarose (Hyclone, Logan, UT, USA) that had been washed three times with pre-chilled PBS (centrifuged for 30 s at 9,000 g and 4°C each time), and incubated on a reciprocating shaker (ABI PE-Applied Biosystems, Foster, CA, USA). The protein samples were centrifuged for 30 s at 9,000 g and 4°C. The supernatant was added to Protein A-Agarose or Protein G-Agarose. It was then incubated overnight at 4°C after addition of the IP antibody. On the following day, protein samples were washed with the IP cell lysis buffer containing 1% protease inhibitor. The supernatant was discarded. An appropriate volume of 2×SDS was added to the sediment. The sediment was then placed in a metal bath for 10 min at 100°C, centrifuged for 10 min, placed in a spacer gel for 30 min at 90 V, and placed in a separation gel for 90–120 min at 120 V. The protein was then transferred to a membrane. Protein was blocked for 1 hr after being transferred to the membrane. Polyvinulidene fluoride (PVDF) membranes were washed with PBS on the reciprocating decoloration shaker following blocking. The primary antibody was added. The source of antibodies was the same as for immunoblotting. Membranes were incubated overnight at 4°C. On the following day, PVDF membranes were washed with PBST for 7 min and 10 min respectively on the reciprocating decoloration shaker. After addition of the secondary antibody, they were incubated for 1 hr at

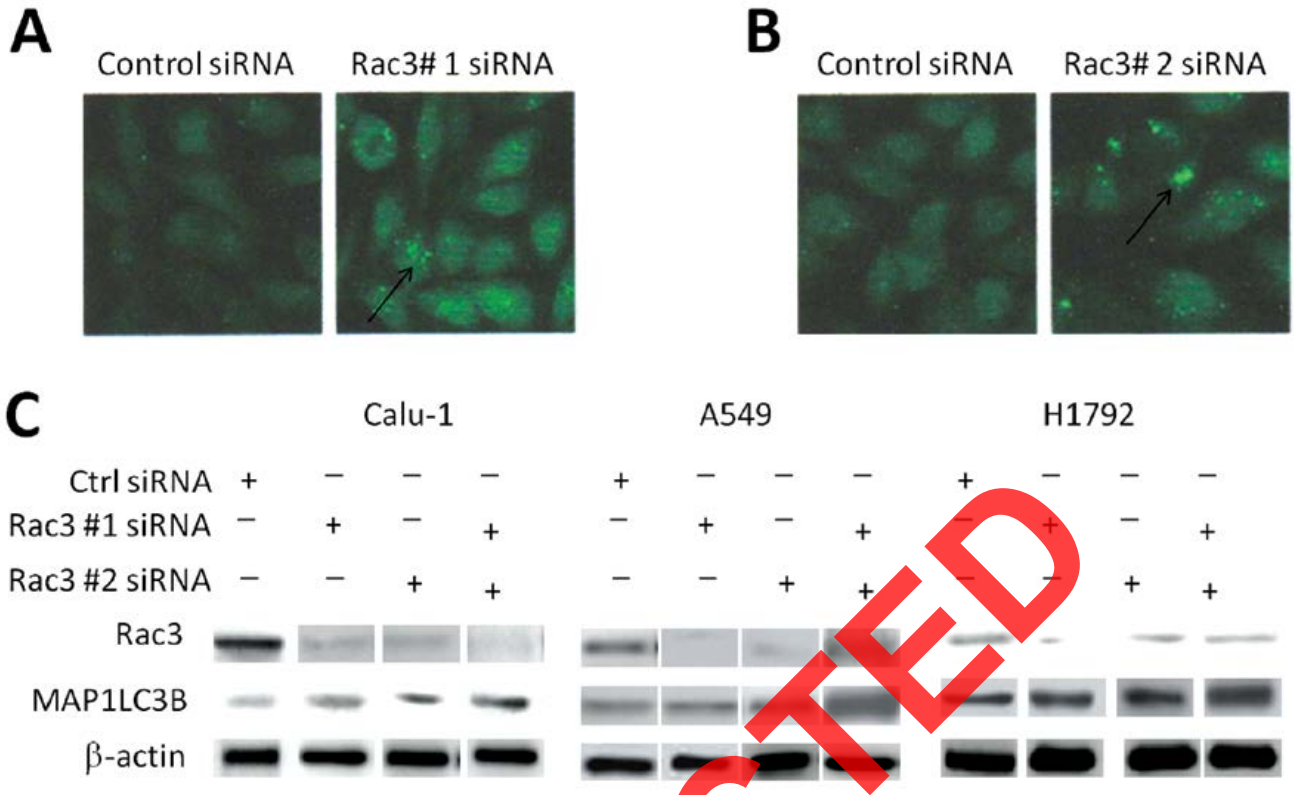

Figure 1. Expression of autophagosomes induced by Rac3 knock-down and the MAP1LC3B protein. **(A)** Expression of the appropriate proteins in the Calu-1-EGFP-MAP1LC3 cells under the spot scanning laser confocal microscope; **(B)** Detection of the expression of intracellular Rac3, MAP1LC3B, and ACTB proteins by immunoblotting at 24 hrs after inhibition of the specific proteins in Calu-1, A549, and H1792 cells with Rac3 siRNA.

room temperature. The PVDF membranes were washed for 10 min, 15 min, and 15 min, respectively, following incubation with the secondary antibody. Membranes were exposed on X-ray film after addition of the chemiluminescent horse radish peroxidase substrate.

Statistics

Five random experimental results were chosen in each experiment. The software GraphPad Prism 5 was used for statistical analysis. All experimental data are expressed as mean ± standard deviation. The SPSS19.0 software was used for statistical analysis of experimental data in various groups. The comparisons of the sample means were by independent sample t-test. The difference was considered statistically significant when $p<0.05$.

Results

Inhibition of Rac3 promotes cell autophagy and the expression of MAPILC3B protein

First, Rac3 siRNA was used to inhibit the expression of the Rac3 protein in Calu-1-EGFP-MAP1LC3 cells. Five fields of view were randomly selected under the spot scanning laser confocal microscope and the average number of bright spots in each cell was counted at 24 hrs after the cells were transfected with siRNA. The statistical results showed that the average number of bright spots in the Rac3 siRNA-treated cells increased significantly compared with the control group (Figure 1A-B). Furthermore, Rac3 siRNA inhibited the expression of specific proteins in Calu-1, A549, and H1792 cells. We observed changes in the expression of the intracellular MAP1LC3B-II protein at 24 hrs after cells were transfected with siRNA. The immunoblotting results demonstrated that the expression of intracellular MAP1LC3B-II protein was upregulated in the Rac3 siRNA-treated cells compared with the control group (Figure 1C).

Autophagy is induced through the ATF4-DDIT4-MTOR signaling pathway after Rac3 knock-down

Next, we measured the expression of intracellular p-RPS6KB1, p-EIF4EBP1, ATF4, and DDIT4 at 24 hrs after inhibiting the expression of Rac3 in Calu-1 and A549 cells using Rac3 siRNA. The results indicated that the expression of the four proteins decreased following inhibition of Rac3 (Figure 2A). The changes in intracellular DDIT4 protein were detected at 48 hrs after the expression of ATF4 in A549 and Calu-1 cells was inhib-

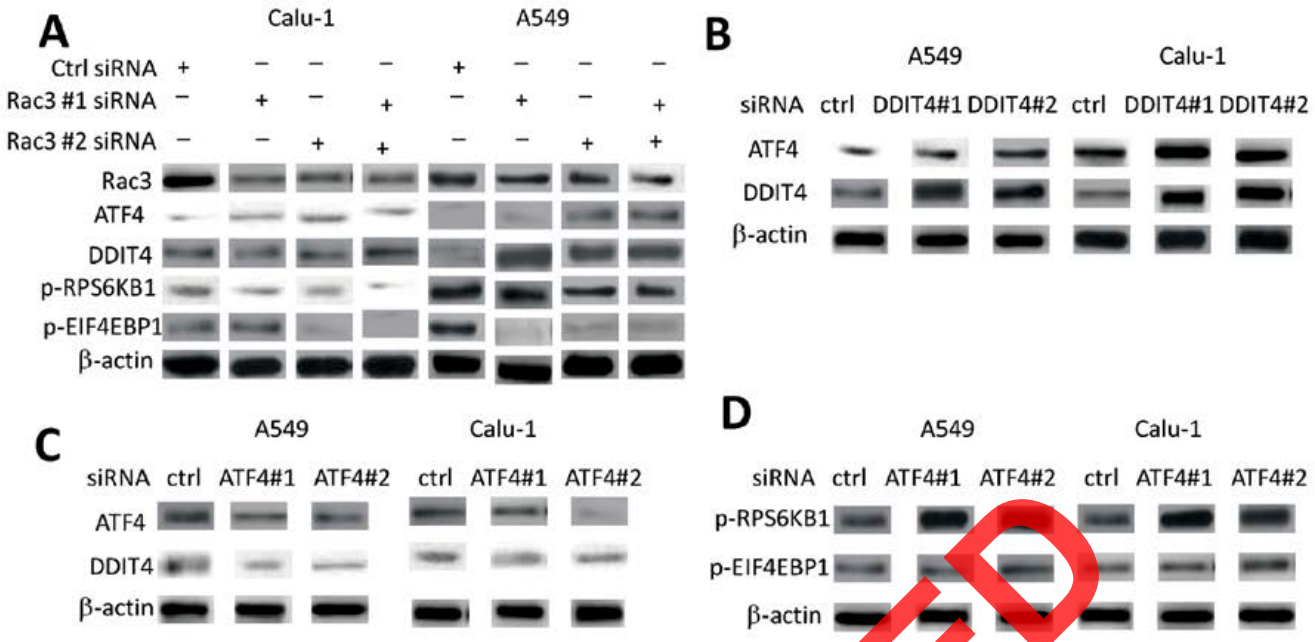

Figure 2. Inducing autophagy through the ATF4-DDIT4-MTOR signaling pathway following Rac3 knock-down. **(A)** Two siRNAs against ATF4 were used to inhibit the expression of the ATF4 in A549 and Calu-1 cells. The expression of Rac3, ATF4, DDIT4, p-RPS6KB1, p-EIF4EBP1, and ACTB proteins in the cells was detected by immunoblotting. **(B)** Two siRNAs against DDIT4 were used to inhibit its gene expression in A549 and Calu-1 cells. The expression of intracellular ATF4 and DDIT4 proteins was detected by immunoblotting. **(C-D)** Two siRNAs against ATF4 were used to inhibit the expression of specific genes in A549 and Calu-1 cells. The expression of intracellular ATF4, DDIT4, p-RPS6KB1, and p-EIF4EBP1 proteins was detected by immunoblotting.

ited by two different siRNA constructs (ATF4 #1 and ATF4 #2) targeting ATF4. The immunoblotting results demonstrated that the expression of DDIT4 decreased significantly after inhibition of ATF4 (Figure 2A). To demonstrate the correlation between the DDIT4 and MTOR signaling pathways in lung cancer cells, the changes in the expression of p-RPS6KB1, p-EIF4EBP1, and MAP1LC3B-II were measured at 48 hrs after two siRNAs targeting DDIT4 (DDIT4 #1 and DDIT4 #2) were used to inhibit the expression of intracellular DDIT4. The results showed that the expression of p-RPS6KB1 and p-EIF4EBP1 was upregulated and the level of the marker of autophagy, MAP1LC3B-II, decreased significantly when intracellular DDIT4 was inhibited (Figure 2B). To demonstrate autophagy of lung cancer cells induced by the ATF4-DDIT4-MTOR signaling pathway following inhibition of Rac3, the changes in the expression of DDIT4, p-RPS6KB1, p-EIF4EBP1, and MAP1LC3B-II were measured at 48 hrs after the expression of ATF4 in A549 and Calu-1 cells was inhibited. The results were consistent with previous observations. The expression of intracellular DDIT4 was significantly downregulated following inhibition of ATF4. Furthermore, the expression of p-RPS6KB1 and p-EIF4EBP1 was upregulated and the expression of MAP1LC3B-II decreased (Figure 2C-D).

Inhibition of Rac3 allows for HSPA5 acetylation and its dissociation from EIF2AK3

The acetylated form of HSPA5 dissociates from EIF2AK3 upstream of ATF4, thus triggering an endoplasmic reticulum stress response [21]. As a member of the deacetylase family, Rac3 is potentially the deacetylase of the molecular chaperone, HSPA5. Therefore, inhibition of Rac3 might increase the degree of HSPA5 acetylation and induce an intracellular endoplasmic reticulum stress response. The cells were treated with the Rac3 siRNA at a concentration of 50 M at 24 hrs after the H1299 and H1792 human non-small cell lung cancer cells were transfected with the plasmid pcDNA3.1-HA-HSPA5. The co-immunoprecipitation results indicated that the bindings of Rac3 and EIF2AK3 to HSPA5 in cells treated with the Rac3 siRNA decreased significantly compared with the control group (Figure 3A). The Calu-1 and H1792 cells were treated with the Rac3 siRNA in the absence of overexpressed HSPA5. It was found that the binding of endogenous HSPA5 to intracellular Rac3 and EIF2AK3 decreased. Furthermore, we detected that the degree of acetylation of intracellular HSPA5 increased (Figure 3B).

The structural domain between HSPA5 and Rac3

The structural domain responsible for acetyl-

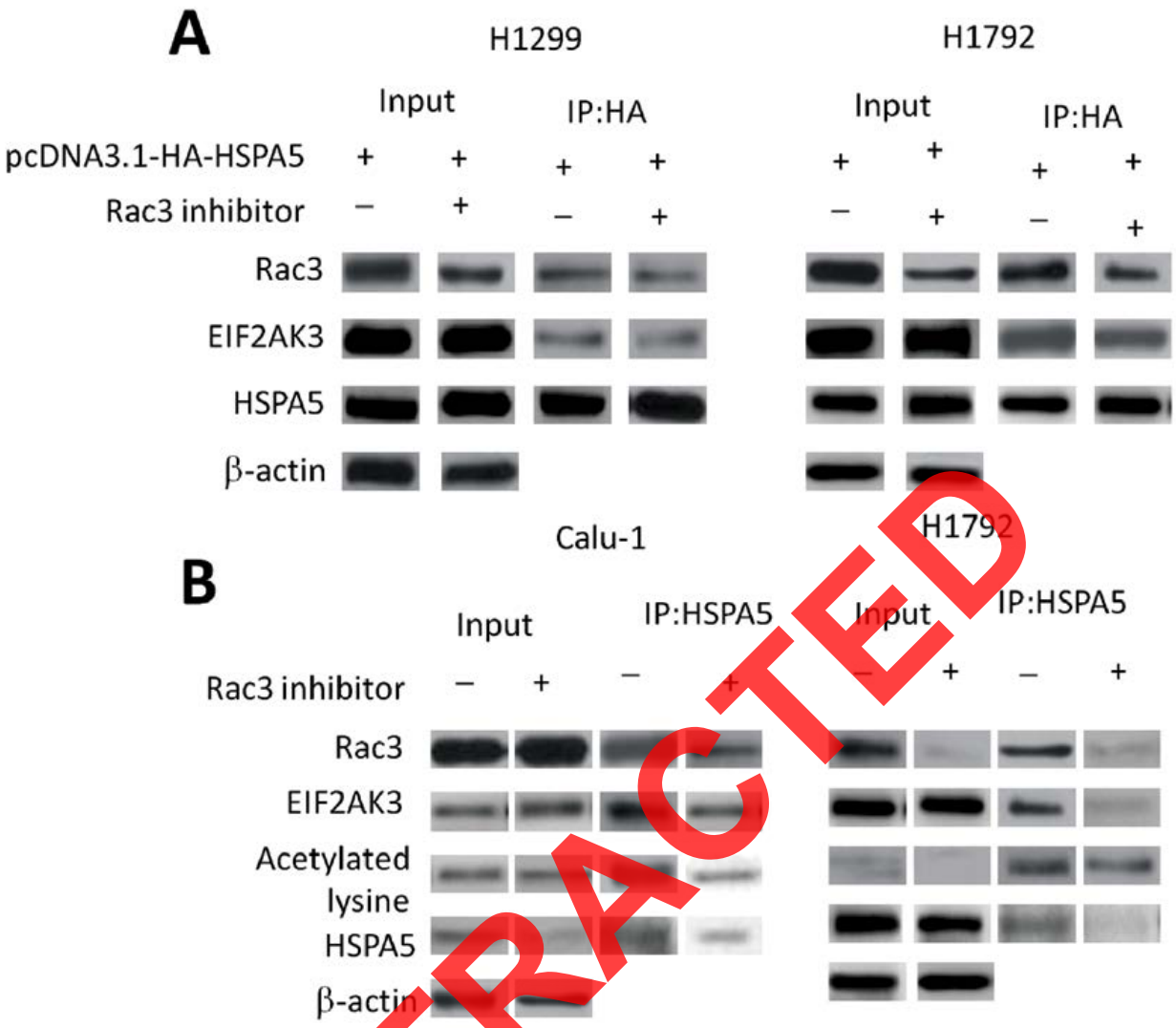

Figure 3. Inhibition of Rac3 allows for dissociation between HSPA5 and EIF2AK3. **(A)** The cells were treated with the Rac3 siRNA for 20 hrs at 2 hrs after H1299 and H1792 cells were transfected with the pcDNA3.1-HA-HSPA5 plasmid. The hemagglutinin (HA) antibody was used for co-immunoprecipitation experiments. The expression of intracellular Rac3, EIF2AK3, HSPA5, and ACTB proteins was detected by immunoblotting. **(B)** Inhibition of Rac3 caused the degree of acetylation of HSPA5 to increase. The IgG or HSPA5 antibody was used for co-immunoprecipitation experiments at 20 hrs after Calu-1 and H1792 cells were treated with the Rac3 siRNA. The expression of intracellular Rac3, EIF2AK3, acetylated lysine, HSPA5, and ACTB proteins was detected by immunoblotting.

ation activity of HSPA5 and Rac3 is the 256-464 (HSPA5) and 65-340 (Rac3) interaction structural domain. The plasmids with full length Rac3 and different structural domains of the HSPA5 protein were co-transfected in 293T cells. The results showed that Rac3 was only bound to the substrate binding structural domains (SBD) of HSPA5 (Figure 4A-B).

Discussion

Autophagy is a metabolic process whereby cells utilize lysosomes to clear or recycle intracellular components for maintaining cellular homeostasis [22]. As it is closely associated with many physiological and pathological processes, it can serve as a possible target for tumor treatment. The aim of the present study was to explore whether the intracellular deacetylase Rac3 can promote autophagy in human non-small cell lung cancer cells after being inhibited, and determine the relationship between autophagy and apoptosis induced by inhibition of Rac3. First, we confirmed the occurrence of autophagy at the cellular level and protein level. Next, we demonstrated that intracellular Rac3 can induce dose- and time-dependent autophagy after being inhibited. Thus, it can be concluded that inhibition of Rac3 in human lung cancer cells can induce autophagy. Many cellular signaling pathways regulate the occurrence of autophagy. The role of the MTOR signaling pathway in regulating autophagy has been thor-

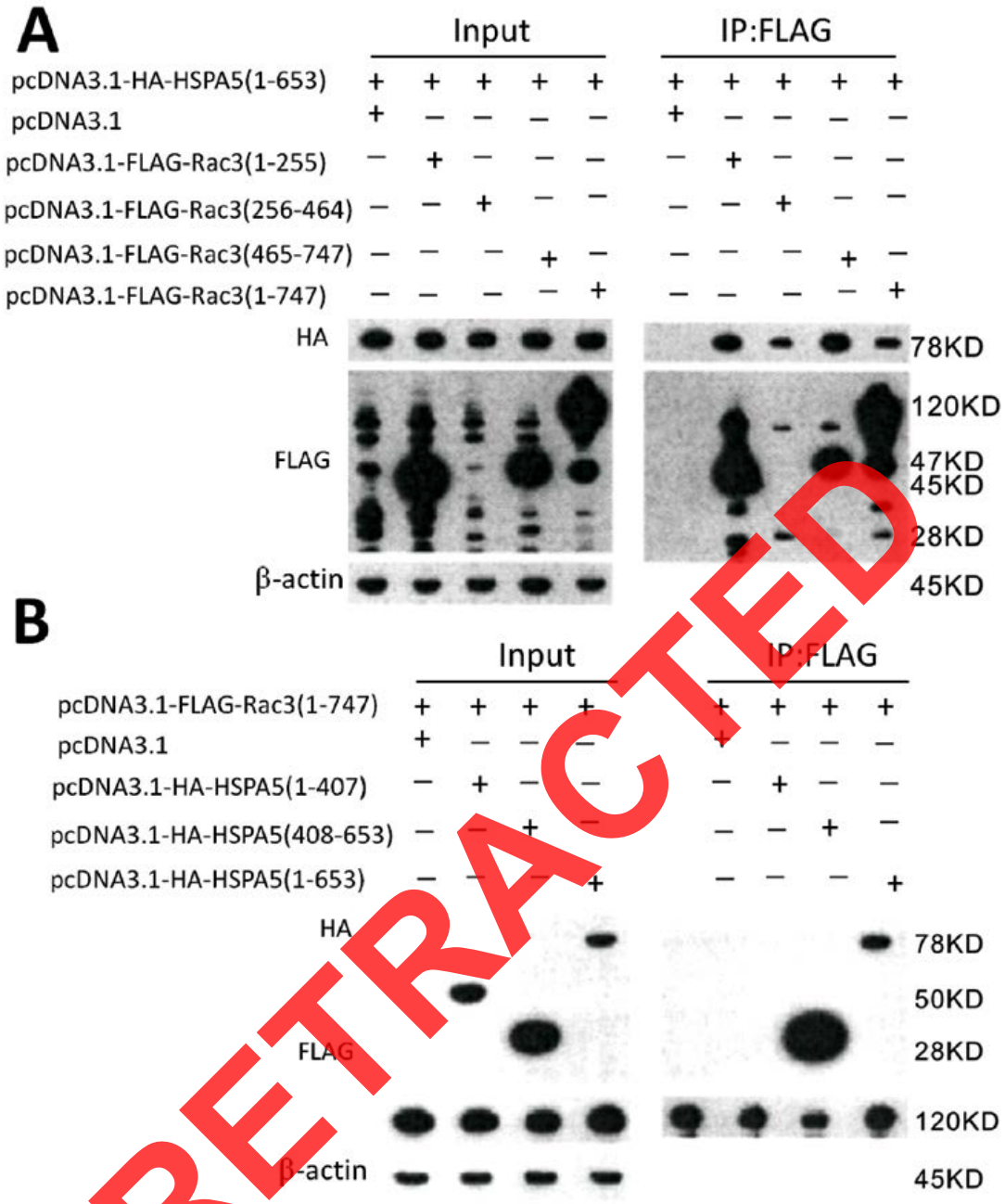

Figure 4. Structural domain involved in the binding of Rac3 to IISPA5. **(A)** Different structural domains represent amino acids of HSPA5 and full length Rac3 protein that were overexpressed in 293FT cells: 1–255, 256–464, 465–747, and Rac3 full length plasmid. The FLAG antibody was used for co-immunoprecipitation experiments. Intracellular hemagglutinin (HA) and FLAG were detected by immunoblotting. **(B)** Different structural domains with full length Rac3 proteins were overexpressed in 293FT cells: 1–407, 408–653, and full length Rac3 plasmids. The FLAG antibody was used for co-immunoprecipitation experiments. Intracellular HA and FLAG were detected by immunoblotting.

oughly reported [4]. Two important downstream proteins of MTORC1 in cells with Rac3 knockdown include p-RPS6KB1 and p-EIF4EBP1 [23]. It was found that the MTORC1 signaling pathway was inhibited by Rac3. According to a previous report, ATF4 can regulate DDIT4, and DDIT4 enables TSC2 to dissociate from 14-3-3, thus inhibiting the MTORC1 signaling pathway [24]. Therefore, the expression of intracellular ATF4 and DDIT4 is detected after Rac3 is inhibited by drugs or siRNA. It was found that the expression of both proteins was upregulated, and the upregulation of DDIT4 occurred slightly later than that of ATF4. This suggests that ATF4 may act upstream of DDIT4 and regulate the expression of DDIT4.

siRNA interference, overexpression of proteins, and spot scanning laser confocal microscopy experiments were employed to determine the specific signaling pathway for autophagy induced by inhibition of Rac3. We found that the upregulation of intracellular ATF4 can cause upregulation of DDIT4, inhibit the MTOR signaling

pathway, and induce cellular autophagy. Cellular autophagy is induced by the ATF4-DDIT4-MTOR signaling pathway following inhibition of Rac3. It is known that the degree of acetylation of the molecular chaperone HSPA5 influences its binding ability to its receptor on the endoplasmic reticulum membrane [25]. We demonstrated that Rac3 is the deacetylase of HSPA5. Therefore, the degree of acetylation of HSPA5 would increase, thus leading to dissociation from EIF2AK3 when the acetylase Rac3 is inhibited. Exposed EIF2AK3 is subject to multimerization and autophosphorylation. Further phosphorylation activates downstream molecules i.e. it activates the endoplasmic reticulum stress response. The intracellular transcription factor ATF4 is upregulated when the endoplasmic reticulum stress response is activated.

We further demonstrated the structural configuration of the binding between HSPA5 and Rac3 using co-immunoprecipitation experiments, with respect to the positioning of HSPA5 and Rac3 in cells and the role of Rac3 as the deacetylase of HSPA5. Based on the experimental results, HSPA5 can bind to all deacetylase-active structural domains of Rac3, which can account for the role of Rac3 in deacetylation of Rac3.

In conclusion, our study demonstrated that inhibition of the deacetylase Rac3 in human lung cancer cells induces autophagy. The reason for the occurrence of autophagy is related to increases in the degree of acetylation of the molecular chaperone HSPA5, thus activating the intracellular ATF4-DDIT4-MTOR signaling pathway. We also further described the structural configuration of binding between HSPA5 and its deacetylase Rac3. We propose a possible method of treatment for non-small cell lung cancer, i.e. combination of a Rac3 siRNA and autophagy inhibitor. This approach would treat cancer by promoting apoptosis of cancer cells.

Conflict of interests

The authors declare no confict of interests.

References

1. Khaminets A, Heinrich T, Mari M et al. Regulation of endoplasmic reticulum turnover by selective autophagy. Nature 2015;522:354-358.
2. Mochida K, Oikawa Y, Kimura Y et al. Receptor-mediated selective autophagy degrades the endoplasmic reticulum and the nucleus. Nature 2015;522:359-362.
3. Palikaras K, Lionaki E, Tavernarakis N. Coordination of mitophagy and mitochondrial biogenesis during ageing in C. elegans. Nature 2015;521:525-528.
4. Diao J, Liu R, Rong Y et al. ATG14 promotes membrane tethering and fusion of autophagosomes to endolysosomes. Nature 2015;520:563-566.
5. Efeyan A, Comb WC, Sabatini DM. Nutrient-sensing mechanisms and pathways. Nature 2015;517:302-310.
6. Venkatanarayan A, Raulji P, Norton W et al. IAPP-driven metabolic reprogramming induces regression of p53-deficient tumours in vivo. Nature 2015;517:626-630.
7. Ejlerskov P, Hultberg JG, Wang J et al. Lack of Neuronal IFN-beta-IFNAR Causes Lewy Body- and Parkinson's Disease-like Dementia. Cell 2015;163:324-339.
8. Miao Y, Li G, Zhang X, Xu H, Abraham SN. A TRP Channel Senses Lysosome Neutralization by Pathogens to Trigger Their Expulsion. Cell 2015;161:1306-1319.
9. Pineda CT, Ramanathan S, Fon TK et al. Degradation of AMPK by a cancer-specific ubiquitin ligase. Cell 2015;160:715-728.
10. Tan X, Thapa N, Sun Y, Anderson RA. A kinase-independent role for EGF receptor in autophagy initiation. Cell 2015;160:145-160.
11. Yan Y, Jiang W, Liu L et al. Dopamine controls systemic inflammation through inhibition of NLRP3 inflammasome. Cell 2015;160:62-73.
12. Wang G, Wang H, Zhang C et al. Rac3 regulates cell proliferation through cell cycle pathway and predicts prognosis in lung adenocarcinoma. Tumor Biol 2016;37:12597-12607.
13. Li J, Liu Y, Yin Y. Inhibitory effects of Arhgap6 on cervical carcinoma cells. Tumour Biol 2016;37:1411-1425.
14. Haataja L, Groffen J, Heisterkamp N. Characterization of RAC3, a novel member of the Rho family. J Biol Chem 1997;272:20384-20388.
15. Ruiz-Lafuente N, Alcaraz-Garcia MJ, Garcia-Serna AM et al. Dock10, a Cdc42 and Rac1 GEF, induces loss of elongation, filopodia, and ruffles in cervical cancer epithelial HeLa cells. Biol Open 2015;4:627-635.
16. Fernandez LP, Ruiz GM, Mengual GD et al. RAC3 more than a nuclear receptor coactivator: a key inhibitor of senescence that is downregulated in aging. Cell Death Dis 2015;6:e1902.
17. Liu TQ, Wang GB, Li ZJ, Tong XD, Liu HX. Silencing of Rac3 inhibits proliferation and induces apoptosis of human lung cancer cells. Asian Pac J Cancer Prev 2015;16:3061-3065.
18. Ciuculescu MF, Park SY, Canty K, Mathieu R, Silberstein LE, Williams DA. Perivascular deletion of murine Rac reverses the ratio of marrow arterioles and sinusoid vessels and alters hematopoiesis in vivo. Blood 2015;125:3105-3113.

19. Wang Y, Kunit T, Ciotkowska A et al. Inhibition of prostate smooth muscle contraction and prostate stromal cell growth by the inhibitors of Rac, NSC23766 and EHT1864. Br J Pharmacol 2015;172:2905-2917.
20. Miyano K, Sumimoto H. Assessment of the role for Rho family GTPases in NADPH oxidase activation. Methods Mol Biol 2015;827:195-212.
21. Finka A, Sharma SK, Goloubinoff P. Multi-layered molecular mechanisms of polypeptide holding, unfolding and disaggregation by HSP70/HSP110 chaperones. Front Mol Biosci 2015;2:29.
22. Lazarou M, Sliter DA, Kane LA et al. The ubiquitin kinase PINK1 recruits autophagy receptors to induce mitophagy. Nature 2015;524:309-314.
23. Tivodar S, Kalemaki K, Kounoupa Z et al. Rac-GTPases Regulate Microtubule Stability and Axon Growth of Cortical GABAergic Interneurons. Cereb Cortex 2015;25:2370-2382.
24. Yang CS, Matsuura K, Huang NJ et al. Fatty acid synthase inhibition engages a novel caspase-2 regulatory mechanism to induce ovarian cancer cell death. Oncogene 2015;34:3264-3272.
25. Shen F, Zhang Y, Yao Y et al. Proteomic analysis of cerebrospinal fluid: toward the identification of biomarkers for gliomas. Neurosurg Rev 2014;37:367-380.